OXFORD

International Journal of Neuropsychopharmacology (2019) 22(1): 57–70

doi:10.1093/ijnp/pyy090
Advance Access Publication: November 8, 2018
Regular Research Article

REGULAR RESEARCH ARTICLE

Emodin Rescued Hyperhomocysteinemia-Induced Dementia and Alzheimer's Disease-Like Features in Rats

Peng Zeng, Yan Shi, Xiao-Ming Wang, Li Lin, Yan-Jun Du, Na Tang, Qun Wang, Ying-Yan Fang, Jian-Zhi Wang, Xin-Wen Zhou, Youming Lu, Qing Tian

Department of Pathology and Pathophysiology, School of Basic Medicine, Tongji Medical College, Huazhong University of Science and Technology, Wuhan, China (Drs Zeng, Shi, Wang, Tang, Ms Qun Wang, Fang, Wang, Zhou, Lu, and Tian); Key Laboratory of Neurological Disease of National Education Ministry and Hubei Province, Institute for Brain Research, Huazhong University of Science and Technology, Wuhan 430030, China (Drs Zeng, Shi, Wang, Tang, Wang, Fang, Ms Qun Wang, Zhou, Lu, and Tian); Hubei University of Traditional Chinese Medicine, Wuhan 430061, China (Drs Lin and Du).

P.Z. and Y.S. contributed equally to this paper.

Correspondence: Dr Youming Lu and Dr Qing Tian, Department of Pathology and Pathophysiology, School of Basic Medicine, Tongji Medical College, Huazhong University of Science and Technology, 13 Hangkong Road, Wuhan 430030, China (lym@hust.edu.cn, tianq@hust.edu.cn).

Abstract

Background: Hyperhomocysteinemia is an independent risk factor for dementia, including Alzheimer's disease. Lowering homocysteine levels with folic acid treatment with or without vitamin B12 has shown few clinical benefits on cognition.
Methods: To verify the effect of emodin, a naturally active compound from *Rheum officinale*, on hyperhomocysteinemia-induced dementia, rats were treated with homocysteine injection (HCY, 400 μg/kg/d, 2 weeks) via vena caudalis. Afterwards, HCY rats with cognitive deficits were administered intragastric emodin at different concentrations for 2 weeks: 0 (HCY-E0), 20 (HCY-E20), 40 (HCY-E40), and 80 mg/kg/d (HCY-E80).
Results: β-Amyloid overproduction, tau hyperphosphorylation, and losses of neuron and synaptic proteins were detected in the hippocampi of HCY-E0 rats with cognitive deficits. HCY-E40 and HCY-E80 rats had better behavioral performance. Although it did not reduce the plasma homocysteine level, emodin (especially 80 mg/kg/d) reduced the levels of β-amyloid and tau phosphorylation, decreased the levels of β-site amyloid precursor protein-cleaving enzyme 1, and improved the activity of protein phosphatase 2A. In the hippocampi of HCY-E40 and HCY-E80 rats, the neuron numbers, levels of synaptic proteins, and phosphorylation of the cAMP responsive element-binding protein at Ser133 were increased. In addition, depressed microglial activation and reduced levels of 5-lipoxygenase, interleukin-6, and tumor necrosis factor α were also observed. Lastly, hyperhomocysteinemia-induced microangiopathic alterations, oxidative stress, and elevated DNA methyltransferases 1 and 3β were rescued by emodin.
Conclusions: Emodin represents a novel potential candidate agent for hyperhomocysteinemia-induced dementia and Alzheimer's disease-like features.

Keywords: homocysteine, emodin, dementia, Aβ, tau

Received: May 12, 2018; **Revised:** November 1, 2018; **Accepted:** November 4, 2018

Significance Statement

Hyperhomocysteinemia (HHcy) is an independent risk factor for dementia, including Alzheimer's disease (AD). In this study, we tested the effect of emodin, a natural active compound from *Rheum officinale*, on HHcy-induced dementia. Emodin rescued HHcy-induced dementia by counteracting the AD-like features including β-amyloid (Aβ) overproduction, tau hyperphosphorylation, neuron loss, synaptic damage, cerebral microvascular damage and inflammation, and alleviating the oxidative stress and methylation impairments in the brains of rats. Our results suggest that emodin represents a novel potential candidate agent for HHcy-induced cognitive deficits.

Introduction

Homocysteine (Hcy) is a crucial intermediate in the metabolism of methionine (Met) to cysteine (Cys) (Prudova et al., 2006). Three pathways are involved in Hcy metabolism: remethylation, transsulfuration, and cyclization (Finkelstein, 1998; Selhub, 1999; Troen, 2005; Kumar et al., 2017). Hcy can be remethylated to Met by methionine synthase enzymes such as 5-methyltetrahydrofolate-homocysteine methyltransferase (remethylation), or it can be metabolized to Cys by cystathionine β-synthase (CBS) and with the help of the cofactors folate, vitamin B12 (Vit B12), and Vit B6 (transsulfuration). Additionally, Hcy can undergo cyclization to form homocysteine thiolactone (cyclization). Elevated Hcy, or hyperhomocysteinemia (HHcy), is mainly due to genetic defects in the Hcy metabolism enzymes such as CBS and methylenetetrahydrofolate reductase or deficiencies of certain cofactors in Hcy metabolism including folate, Vit B6, Vit B12, and choline (Troen et al., 2008a, 2008b; Kumar et al., 2017; 2018). Additionally, several other factors such as pregnancy and lactation are reported to contribute to HHcy (Desouza et al., 2002; Cotter et al., 2003).

HHcy is a risk for dementia, including Alzheimer's disease (AD) and vascular dementia (Obeid et al., 2007; Sharma et al., 2015). Clinical studies concluded that Hcy is associated with the degree of cognitive impairment and acts as a biomarker for the progression of dementia (Kitzlerová et al., 2014). Previously, we reported the correlation between higher plasma Hcy levels with cognition deficits and AD-like features including β-amyloid (Aβ) overproduction and tau hyperphosphorylation in the hippocampi of HHcy rats (Zhang et al., 2008; 2009).

Supplements of Vit B12 and folate are regarded as effective Hcy-lowering interventions (Malouf et al., 2003; de Koning et al., 2016). However, studies from the trials (Fioravanti et al., 1998; Clarke et al., 2003; Sommer et al., 2003) reported that folate with or without Vit B12 did not improve any measures of cognition or mood for healthy, cognitively impaired or demented people in comparison with placebo (Malouf et al., 2003). This outcome suggests that HHcy induces brain disorders by direct harmful manners via vascular and/or neurotoxic pathophysiologic mechanisms (Kamat et al., 2015). Thus, new drugs with new targets are needed to treat HHcy-initiated brain disorders.

Rheum officinale is the most important herb in some prescriptions of traditional Chinese medicine with brain protection features, such as *Tiao-wei-cheng-qi* decoction, *Da-cheng-qi* decoction, etc. (Gong et al., 2011). Emodin (1,3,8-trihydroxy-6-methylanthraquinone), a natural active compound extracted from *Rheum officinale*, has multiple biological activities such as antiinflammation, antioxidant, anticancer, and so on (Huang et al., 1991; Srinivas et al., 2007; Yiu et al., 2014). To explore the effect of emodin on HHcy-induced dementia, 52 rats with cognitive deficits induced by Hcy (HCY rats) were administered emodin treatment at different concentrations: 0 (HCY-E0), 20 (HCY-E20), 40 (HCY-E40), and 80 mg/kg/d (HCY-E80). Two weeks later, HCY-E40 and HCY-E80 rats had better performances in novel object recognition and spatial cognition tests than HCY-E0 rats. Further, emodin treatment improved AD-like features including Aβ overproduction, tau hyperphosphorylation, neuron loss, synaptic impairments, cerebral microvascular damage, and inflammation, and it alleviated oxidative stress and methylation impairments. Our results suggest that emodin represents a novel potential candidate agent for HHcy-induced dementia.

Materials and Methods

Drugs and Antibodies

Hcy from Sigma (St. Louis, MO) was dissolved in normal saline (NS) (400 μg/mL) and filtered before injection. Emodin was obtained from Shanghai Base Industry (Shanghai, China) and dissolved in 0.5% carboxymethylcellulose sodium, which was from Xilong Chemical (Guangzhou, China). The sandwich enzyme-linked immunosorbent assay (ELISA) kit for Hcy was purchased from Mosak Biotechnology (Wuhan, China), and the ELISA kits for Aβ40, Aβ42, malondialdehyde (MDA), superoxide dismutase 1 (SOD1), interleukin-6 (IL-6), and tumor necrosis factor α (TNF-α) were from Elabscience Biotechnology (Wuhan, China). The antibodies used are listed in Table 1.

Animals and Treatments

Sprague-Dawley rats (2 months old, 280±10 g) were obtained from the Disease Control and Prevention Center of Hubei Province (Wuhan, China). All rats received food and water ad libitum in a standard animal house, with a 12-hour-light/-dark cycle with the lights on from 7:00 AM to 7:00 PM, relative humidity (55±15%), and a constant room temperature (22±2°C). All experiments in this study were performed according to the Policies on the Use of Animals and Humans in Neuroscience Research revised and approved by the Society for Neuroscience in 1995.

Sixty-five male rats were randomly divided into 2 groups: 52 rats were administered 2 weeks of Hcy injections (400 μg/kg/d, via vena caudalis, HCY rats) as previously reported (Zhang et al., 2008; 2009), and 13 rats were administered NS injections (CON rats) in the same volume as the Hcy treatments (Figure 1A). The injections were performed with an insulin syringe (29 gauge, 0.33×12.7 mm) at 9:00 AM every day. After the final injection, the animals completed the open field test (OFT) and novel object recognition test (NORT) to assess their locomotor and cognitive activities. In the preliminary experiments, we observed that intragastric administrations of 100 and 120 mg/kg/d emodin induced obvious weight loss and liquid stool in adult SD male rats. Therefore, HCY rats were randomly divided into 4 groups (HCY-E0, HCY-E20, HCY-E40, and HCY-E80, n=13/group) to receive intragastric administrations of emodin at different concentrations (e.g., 0, 20, 40, and 80 mg/kg/d). These administrations were performed from 9:00 AM to 12:00 PM every day. HCY-E0 rats were administered a vehicle (0.5% carboxymethylcellulose sodium). Two weeks later, all rats

Table 1. Antibodies Used in This Study

Antibody	Epitopes	mAb/pAb	Dilution	Source
DM1A	α-tublin	mAb	1:2000 for WB	Sigma (St. Louis, MO)
β-actin	Total β actin	mAb	1:1000 for WB	Abcam (Cambridge, UK)
pCREB	p-CREB at Ser133	pAb	1:1000 for WB	Cell Signaling (Danvers, MA)
CREB	Total CREB	pAb	1:1000 for WB	Cell Signaling (Danvers, MA)
DNMT1	Total DNMT1	pAb	1:400 for WB	Boster Biological Technology (Wuhan, China)
DNMT3α	Total DNMT3α	mAb	1:200 for WB	Boster Biological Technology (Wuhan, China)
DNMT3β	Total DNMT3β	mAb	1:200 for WB	Boster Biological Technology (Wuhan, China)
GluR1	Total GluR1	pAb	1:1000 for WB	Millipore (Billerica, MA)
NR1	Total NR1	pAb	1:1000 for WB	Chemicon
NR2B	Total NR2B	pAb	1:1000 for WB	Abcam (Cambridge, UK)
Synaptophysin	SYP 245–258	pAb	1:1000 for WB	Abcam (Cambridge, UK)
Synapsin1	Synapsin1 C-term	pAb	1:1000 for WB	Abcam (Cambridge, UK)
NF-κB p65	p-NF-κB p65 at Ser536	pAb	1:1000 for WB	Cell Signaling (Danvers, MA)
Iba1	A marker of microglia	pAb	1:200 for IHC	Wako (Osaka, Japan)
RECA-1	Rat endothelial cell surface antigen	mAb	1:50 for IHC	AbD Serotec (Oxford, UK)
BACE1	BACE C-15	pAb	1:500 for WB	Santa Cruz
Tau1	np-tau at Ser-198/199/202	mAb	1:1000 for WB 1:200 for IHC	Chemicon (Temecula, CA)
Tau5	Total tau	mAb	1:500 for WB	Millipore (Billerica, MA)
pT231	p-tau at Thr231	pAb	1:1000 for WB	Biosource (Camarillo, CA)
pS396	p-tau at Ser396	pAb	1:1000 for WB	Biosource (Camarillo, CA)
pS214	p-tau at Ser214	pAb	1:500 for WB	Biosource (Camarillo, CA)
5-LO	Total 5 Lipoxygenase	mAb	1:1000 for WB 1:100 for IHC	Abcam (Cambridge, UK)
PP2Ac	PP-2A catalytic subunit	pAb	1:1000 for WB	Biosource (Camarillo, CA)
p-PP2Ac	p-PP2A at Tyr307	pAb	1:1000 for WB	Santa Cruz
DM-PP2Ac	Demethylated PP2A at Leu309	pAb	1:1000 for WB	Abcam (Cambridge, UK)

Abbreviations: IHC, immunohistochemistry; mAb, monoclonal antibody; np-, non-phosphorylated; p-, phosphorylated; pAb, polyclonal antibody; WB, western blotting.

completed the NORT and Morris water maze test (MWMT). All behavioral tests were performed during the light period.

OFT

Before tests, rats were placed in the specialized testing room for 1 hour of habituation. The floor of the chamber was divided into 25 equal squares with lines, and the arena was cleaned with 75% alcohol after every test. The rat was placed in the center of an open-field arena for 5 minutes, and its behaviors were recorded by an overhanging camera. The zone crossing times were used to assess the general locomotor activities of rats.

NORT

NORT is widely used to assess recognition memory in rodents (Broadbent et al., 2010). On the 1st day (acquisition trial), 2 identical objects were placed in opposite corners of the testing chamber, and the rat was placed in the chamber to explore the objects for 10 minutes. The behaviors were recorded with an overhanging camera. On the 2nd day (retention trial), a distinctly different novel object and one of the original objects in the same location were placed in the chamber. Each rat was allowed to explore the objects for 5 minutes. For the acquisition trial, the recognition index (RI) was calculated as the percentage of time spent exploring one object of the total exploring time. The RI in the retention trial was calculated as the percentage of time spent exploring the novel object over the whole exploring time.

MWMT

The spatial cognition abilities of rats were evaluated by MWMT (Morris, 1984). For learning, rats were trained in the water maze to find a hidden platform for 5 consecutive days (4 trials/d). In each trial, the test ended when the animals climbed onto the platform. If the rats failed to find the hidden platform within 60 seconds, they were manually guided to the platform and remained there for 30 seconds. The rats were allowed 1 day of rest before the memory test, in which the platform was removed. The escape latencies, the numbers of platform crossings, and the swimming speed were monitored by a computerized tracking system.

Western Blotting and ELISA

Rats were anesthetized with isoflurane and killed. The hippocampi were rapidly harvested on ice and stored at –80°C. For Western blotting, the hippocampi were homogenized at 4°C using a homogenizer in 50 mM Tris-HCl (pH 7.4), 150 mM NaCl, 10 mM NaF, 1 mM Na_3VOE_4, 5 mM EDTA, 2 mM benzamidine, and 1 mM phenylmethylsulfonyl fluoride. The extract was mixed with sample buffer (3:1, v/v) containing 200 mM Tris-HCl, pH 7.6, 8% SDS, 40% glycerol, and 40 mM dithiothreitol boiled for 10 minutes and then centrifuged at 12 000 × g for 10 minutes at 25°C. The supernatant was stored at –80°C. Protein concentrations were measured using a bicinchoninic acid kit (Thermo Fisher Scientific, Waltham, MA). The proteins were separated by 8% or 10% sodium dodecyl sulphate polyacrylamide gel electrophoresis and transferred onto nitrocellulose membranes, and then the membranes were blocked with 5% nonfat milk dissolved in Tris-buffered saline (TBS) for 1 hour and probed with primary antibodies for 18 hours. The membranes were washed with TBS-Tween-20 and incubated with anti-rabbit or anti-mouse IgG conjugated to IRDye-800 CW (1:15 000) for 1 hour at 25°C. After washing with TBS-Tween-20, the membranes were

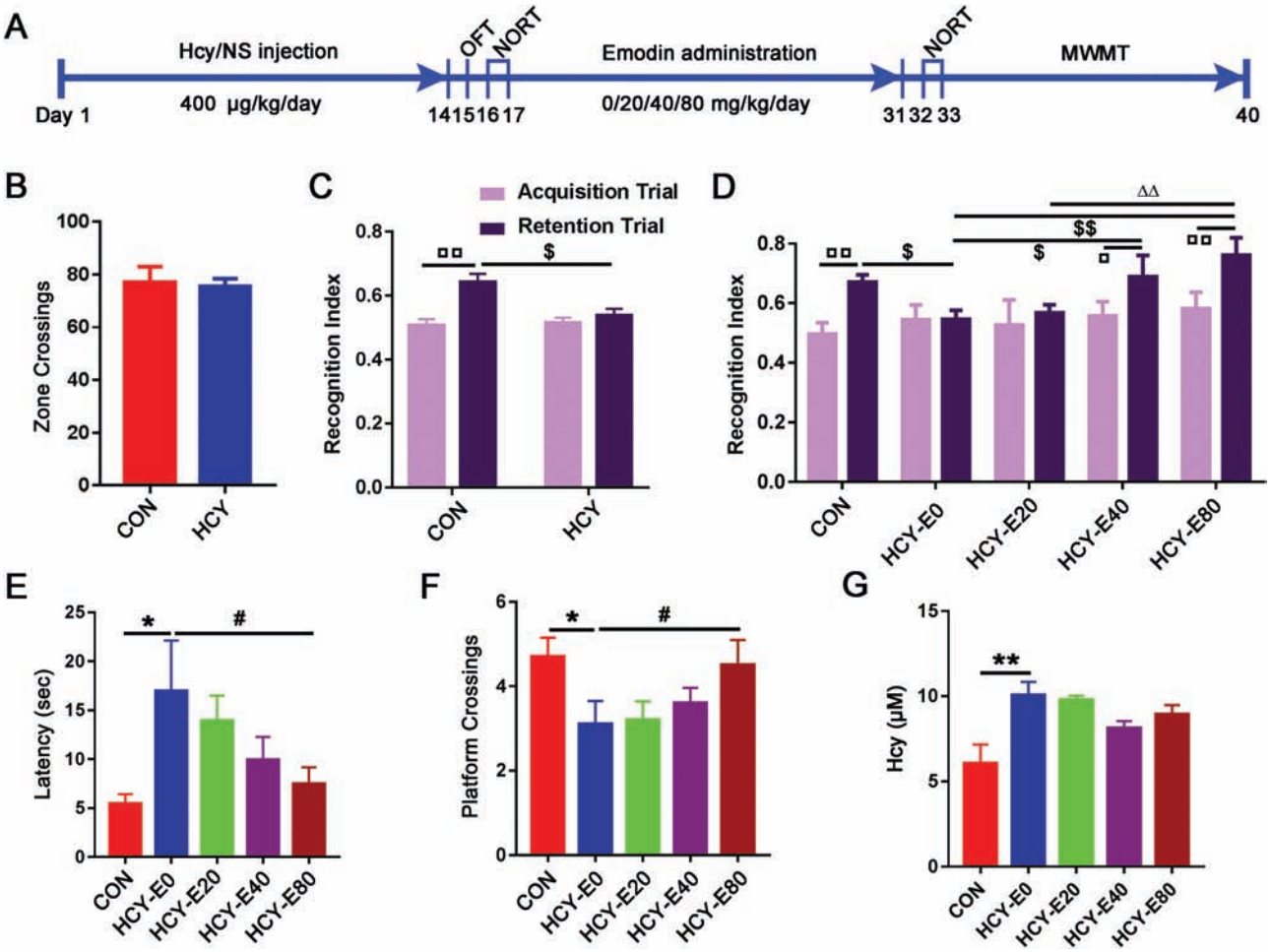

Figure 1. Cognitive deficits in homocysteine-injected rats were rescued by emodin. The experimental workflow is shown in (A). Sixty-five male rats were randomly divided into 2 groups, 52 rats were administered 2 weeks of homocysteine (Hcy) injections (400 μg/kg/d, via the vena caudalis, HCY rats, n = 52), and 13 rats were administered normal saline (NS) injections (control [CON] rats, n = 13) in the same volume as the Hcy treatment. The injections were performed with an insulin syringe (29 gauge, 0.33 × 12.7 mm) at 9:00 AM every day. After the final injection, the animals completed the open field test (OFT) and novel object recognition test (NORT) to assess their activities of locomotion and cognition. The numbers of zone crossings in OFT (B) and the recognition indexes (RI) during the acquisition trial and retention trial in NORT (C) of HCY and CON rats were recorded. Then, HCY rats were randomly divided into 4 groups (HCY-E0, HCY-E20, HCY-E40, and HCY-E80, n = 13/group) to be administered intragastric emodin at different concentrations (e.g., 0, 20, 40, and 80 mg/kg/d, respectively). HCY-E0 rats received a vehicle control (0.5% carboxymethylcellulose sodium). Two weeks later, the RI during the acquisition trial and retention trial in NORT (D), the escape latencies on the 5th day in the learning phase (E), and the times crossing the platform in the memory tests in Morris water maze (F) of the rats were recorded. The plasma Hcy levels of the rats were detected by ELISA (n = 4) (G). Data were expressed as the means ± SEM. $^{□}P < .05$, $^{□□}P < .01$, vs the data of same rats in acquisition trial. $^{$}P < .05$, $^{$$}P < .01$ vs HCY-E0 (HCY). $^{\Delta\Delta}P < .01$ vs HCY-E20. $^{*}P < .05$, $^{**}P < .01$ vs CON. $^{\#}P < .05$ vs HCY-E0.

visualized and quantitatively analyzed by an Odyssey infrared imager system (Li-Cor Bioscience).

The hippocampal levels of Aβ40, Aβ42, IL-6, TNF-α, MDA, and SOD1 and plasma levels of Hcy, IL-6, and TNF-α were assayed by ELISA. The hippocampi were homogenized in phosphate-buffered saline (PBS) (0.01 M) on ice and centrifuged for 5 minutes at 5000 × g to obtain the supernatant. Blood samples were drawn from a heart puncture and promptly centrifuged at 2000 × g for 15 minutes at 4°C. The blood or hippocampal supernatants were incubated in the ELISA microplate for 90 minutes at 37°C. After adding the stop solution, the optical densities were measured by a BioTek Synergy 2 microplate reader (Winooski, VT).

Brain Slice Preparation and Immunohistochemical, Nissl, and HE Stainings

Rats were anaesthetized and sacrificed with an over-dose of isoflurane and immediately perfused with 100 mL of NS followed by 400 mL of 4% paraformaldehyde solution. To visualize the cerebral vasculature, fluorescein isothiocyanate (FITC) was used as reported (Miyata and Morita, 2011). Briefly, the rats received intracardiac perfusion with FITC-containing NS at pH 7.0 followed by paraformaldehyde fixative at pH 8.0. The brains were dissected and post-fixed in perfusate overnight at 4°C. After being dehydrated twice in 30% sucrose in PBS, brains were cut into coronal slices (24 μm) with a freezing microtome (Leica). The brain slices were collected consecutively in PBS.

For immunohistochemistry staining, free-floating slices were blocked with 0.3% H_2O_2 in absolute methanol (30 minutes) and nonspecific sites were blocked with bovine serum albumin (30 minutes). The slices were then incubated overnight at 4°C with primary antibodies (see Table 1). After washing with PBS, the slices were subsequently incubated with biotin-labelled secondary antibodies for 1 hour at 37°C. The immunoreaction was detected using horseradish peroxidase-labelled antibodies and visualized with the diaminobenzidine tetrachloride system. For

each primary antibody, 3 to 5 consecutive slices from each brain were used. For Nissl staining, the slices were washed twice for 5 minutes in 0.01 M PBS and incubated in 0.1% toluidine blue staining solution for 10 minutes at room temperature. Then they were rinsed in distilled water, soaked in 95% ethanol for 10 minutes, and dehydrated in 100% ethanol. After dehydration, the slices were cleared in xylene. For HE staining, the slices were stained with haematoxylin and eosin after being immersed in distilled water for 3 minutes. Then they were dehydrated through increasing concentrations of ethanol and xylene. All slices were covered with neutralized resin. The images were acquired with the same parameters by a microscope (Olympus SV120, Tokyo, Japan).

Statistical Analysis

Statistical analysis was performed using SPSS 12.0 (SPSS Inc., Chicago, IL). The data were expressed as the means ± SEM. The 1-way ANOVA procedure followed by Tukey's multiple comparisons test was used to determine the differences between groups. For the 2 group comparisons, the data were analysed statistically using the *t* test. The level of significance was defined as $P < .05$.

Results

Cognitive Deficits of HCY Rats Were Rescued by Emodin

HCY and CON rats had equivalent zone crossing in OFT ($t_{63} = 0.2703$, $P = .7878$, independent *t* test; Figure 1A–B) and equal RI levels in the acquisition trial of NORT ($t_{63} = 0.2193$, $P = .8271$, independent *t* test; Figure 1C). In the retention trial of NORT, the CON rats showed a higher RI (0.64 ± 0.03) than the HCY rats (0.54 ± 0.02) ($t_{63} = 2.295$, $P = .0251$, independent *t* test; Figure 1C). After 2 weeks of emodin treatments, the rats were subjected to the behavior tests again (Figure 1A). In NORT, RIs of the HCY-E40 (0.69 ± 0.07) and HCY-E80 (0.76 ± 0.06) rats in the retention trial were significantly increased compared with the acquisition trial (0.56 ± 0.05 and 0.58 ± 0.05, respectively) ($t_{24} = 2.086$, $P = .0478$, paired *t* test, HCY-E40; $t_{24} = 2.233$, $P = .0351$, paired *t* test, HCY-E80; Figure 1D), showing that HCY-E40 and HCY-E80 rats had more interest in the novel object as CON rats. On the 5th day of learning in MWMT, the HCY-E0 rats had the longest latency (17.0 ± 5.2 seconds) to find the submerged platform [$F_{(4, 60)} = 5.307$, $P = .001$; Figure 1E], while the latency in the HCY-E80 rats was 7.5 ± 1.7 seconds and in CON rats was 5.5 ± 1.0 seconds. In the memory testing, both the CON (4.7 ± 0.45) and HCY-E80 rats (4.5 ± 0.6) had more crossing times than the HCY-E0 rats (3.1 ± 0.55) [$F_{(4, 60)} = 4.114$, $P = .0052$; Figure 1F]. The moving speeds of rats in OFT, NORT, and MWMT showed no difference. All these data suggested that emodin treatment (40, 80 mg/kg/d) significantly improved the cognitive deficits of HHcy rats. The plasma Hcy levels were detected after behavior tests. HCY-E0 rats had higher Hcy levels (10.1 ± 0.8 μM) than CON rats (6.1 ± 1.1 μM), while the Hcy levels in HCY-E40 (8.1 ± 0.4 μM) and HCY-E80 (8.9 ± 0.6 μM) rats decreased slightly [$F_{(4, 15)} = 5.384$, $P = .0068$; Figure 1G].

Emodin Increased Hippocampal Neurons and Synapse-Related Proteins

Nissl staining was used to show the neuron numbers in the hippocampi (Figure 2A). Decreased neurons were observed in the CA3 region of the HCY-E0 rats (approximately 86.5% of the CON rats) [$F_{(4, 25)} = 7.406$, $P = .0004$; Figure 2B], but this difference was not observed in the CA1, CA2, and dentate gyrus regions. The neuron numbers of the CA3 region in the HCY-E40 and HCY-E80 rats were increased compared with the HCY-E0 rats (Figure 2B). cAMP responsive element-binding protein (CREB) is a nuclear transcription factor essential for memory formation and retention, and its activation primarily depends on the phosphorylation at Ser133 (pCREB) (Shaywitz and Greenberg, 1999). The hippocampal pCREB level in the HCY-E0 rats was only 26.3% of the CON rats. Both the HCY-E40 (49.7% of CON) and HCY-E80 (81.7% of CON) rats had higher pCREB levels than the HCY-E0 rats [$F_{(4, 25)} = 41.54$, $P < .0001$; Figure 2C–D].

Synapses propagate electrical or chemical signals between neurons. Here, the hippocampal presynaptic proteins (synapsin 1 and synaptophysin) and postsynaptic proteins [glutamate receptor 1 (GluR1), N-methyl D-aspartate receptor (NR) subtype 1 (NR1) and NR2B] were detected (Figure 2E–G). The HCY-E0 rats had significantly decreased GluR1 (58.5%, $F_{(4, 25)} = 3.037$, $P = .036$), NR1 (44.8%, $F_{(4, 25)} = 7.77$, $P = .0003$), synaptophysin (48.1%, $F_{(4, 25)} = 6.422$, $P = .0011$), and synapsin 1 (48%; $F_{(4, 25)} = 13.02$, $P < .0001$) levels, while NR2B levels were unchanged. Compared with the HCY-E0 rats, HCY-E40 had increases of 107.2% in NR1, 67.3% in synaptophysin, and 125.9% in synapsin 1 levels, and HCY-E80 rats had increases of 138.4% in GluR1, 108.2% in NR1, 50.2% in NR2B, 44.2% in synaptophysin, and 256.3% in synapsin 1 levels (Figure 2E–G). These data suggested that emodin may attenuate HHcy-induced loss of neurons and synaptic proteins.

Emodin Eliminated Hippocampal Aβ Overproduction and Tau Hyperphosphorylation

By ELISA, higher levels of hippocampal Aβ40 (4496 ± 248 pg/g tissue) and Aβ42 (905.5 ± 42 pg/g tissue) were found in the HCY-E0 rats compared with the CON rats (Aβ40, 3439 ± 190; Aβ42, 689.5 ± 35 pg/g tissue) [$F_{(4, 25)} = 6.751$ for Aβ40, $P = .0008$; $F_{(4, 25)} = 4.618$ for Aβ42, $P = .0063$; Figure 3A–B]. Decreased Aβ40 levels in the HCY-E20, HCY-E40, and HCY-E80 rats and decreased Aβ42 in the HCY-E80 rats (621.9 ± 82 pg/g tissue) (Figure 3A–B) were observed. Significantly decreased β-site amyloid precursor protein-cleaving enzyme 1 (BACE1), the rate-limiting enzyme for Aβ production, was found in the HCY-E40 (147.3% of CON) and HCY-E80 rats (139.3% of CON) [$F_{(4, 25)} = 8.714$, $P = .0002$] (Figure 3C–D).

In the HCY-E0 rats, the levels of hippocampal tau phosphorylated at Thr231 (pT231), Ser396 (pS396), and Ser214 (pS214) were significantly increased (187%, 213%, and 195% of CON, respectively), and the level of tau unphosphorylated at Ser198/199/202 (Tau1) was significantly decreased (52.3% of CON) [$F_{(4, 25)} = 21.31$ for Tau1, $P < .0001$; $F_{(4, 25)} = 9.788$ for pT231, $P < .0001$; $F_{(4, 25)} = 31.92$ for pS396, $P < .0001$; $F_{(4, 25)} = 13.41$ for pS214, $P < .0001$; Figure 3E–F). In the HCY-E20, HCY-E40, and HCY-E80 rats, the levels of tau phosphorylation at Thr231, Ser396, Ser214, and Ser198/199/202 were significantly decreased. The immunohistochemical staining with Tau1 on brain slices confirmed the results [$F_{(4, 25)} = 17.89$, $P < .0001$; Figure 4E–F]. Total tau showed no differences (Tau5, Figure 3E–F).

Protein phosphatase 2A (PP2A) is involved in HHcy-induced Aβ overproduction and tau hyperphosphorylation (Zhang et al., 2008, 2009). In the HCY-E0 rats, significantly increased levels of Leu309-demethylation (DM-PP2Ac, 157.1% of CON) and Tyr307-phosphorylation (p-PP2Ac, 133.6% of CON) of the PP2A catalytic subunit (PP2Ac) [$F_{(4, 25)} = 0.1303$ for PP2Ac, $P = .9699$; $F_{(4, 25)} = 4.978$ for p-PP2Ac, $P = .0043$; $F_{(4, 25)} = 6.849$ for DM-PP2Ac, $P = .0007$; Figure 3G–H] were observed, indicating the inhibition of PP2A.

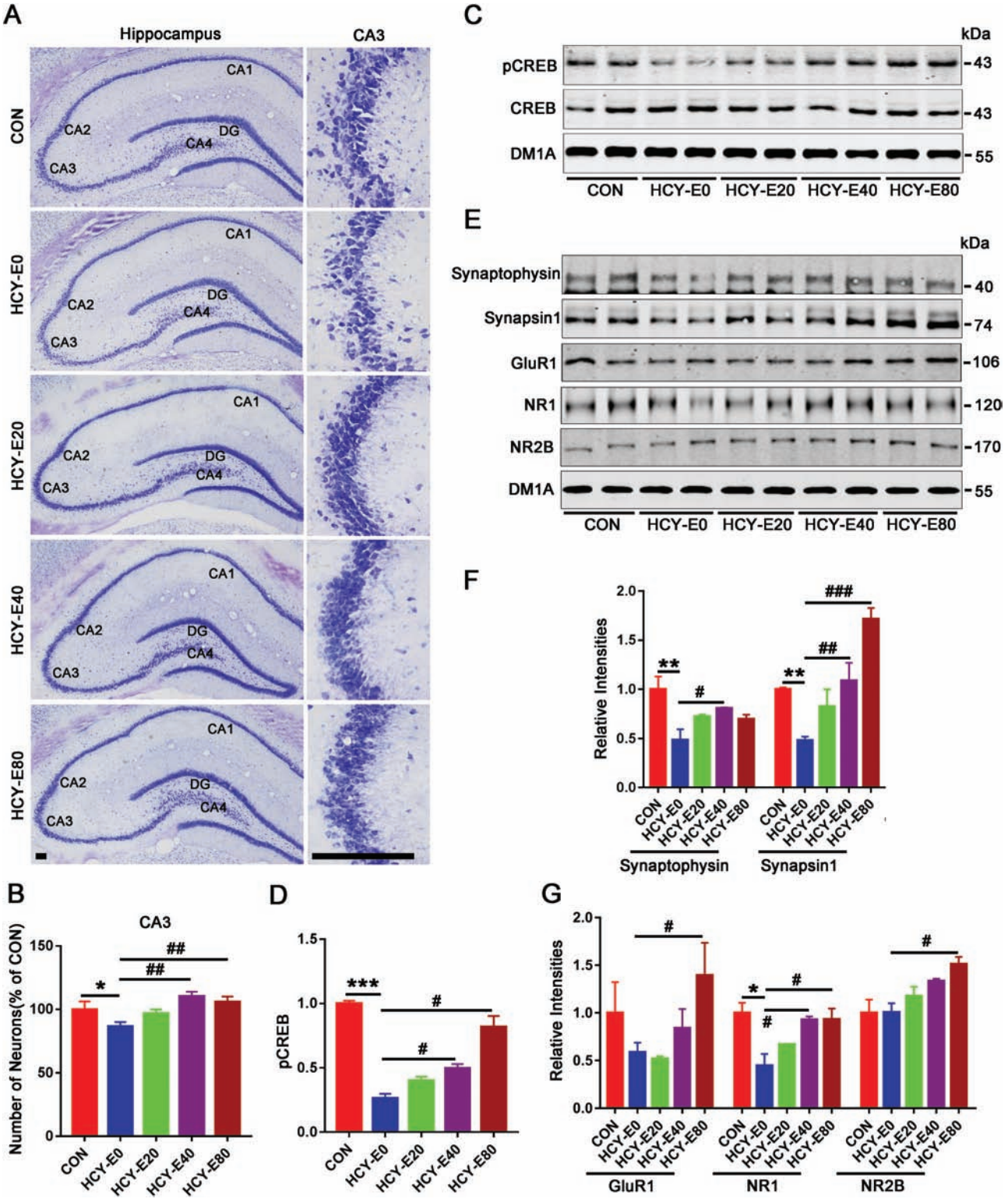

Figure 2. Hippocampal neurons and synapse-related proteins. Neurons in the CA1, CA2, CA3, CA4, and dentate gyrus regions of the hippocampi were detected with Nissl staining (A, bar = 50 μm) and quantified by ImageJ. Differences were only found in the numbers of neurons in the CA3 region (B, n = 6). Levels of CREB, its phosphorylation at S133 (pCREB) (C–D), and synaptic proteins including synaptophysin, synapsin1, glutamate receptor 1 (GluR1), N-methyl D-aspartate receptor (NR) subtype 1 (NR1), and NR2B (E–G) were measured by western blotting and quantitatively analyzed (n = 6). Data were expressed as the means ± SEM. $^{*}P < .05$, $^{**}P < .01$, $^{***}P < .001$ vs CON. $^{\#}P < .05$, $^{\#\#}P < .01$, $^{\#\#\#}P < .001$ vs HCY-E0.

In the HCY-E40 and HCY-E80 rats, the levels of DM-PP2Ac and p-PP2Ac were obviously reduced. Analysis of total PP2Ac levels showed no differences (Figure 3G–H). We also measured the activation of glycogen synthase kinase 3β, a key kinase activated in AD processing, but no alterations were observed (data not shown).

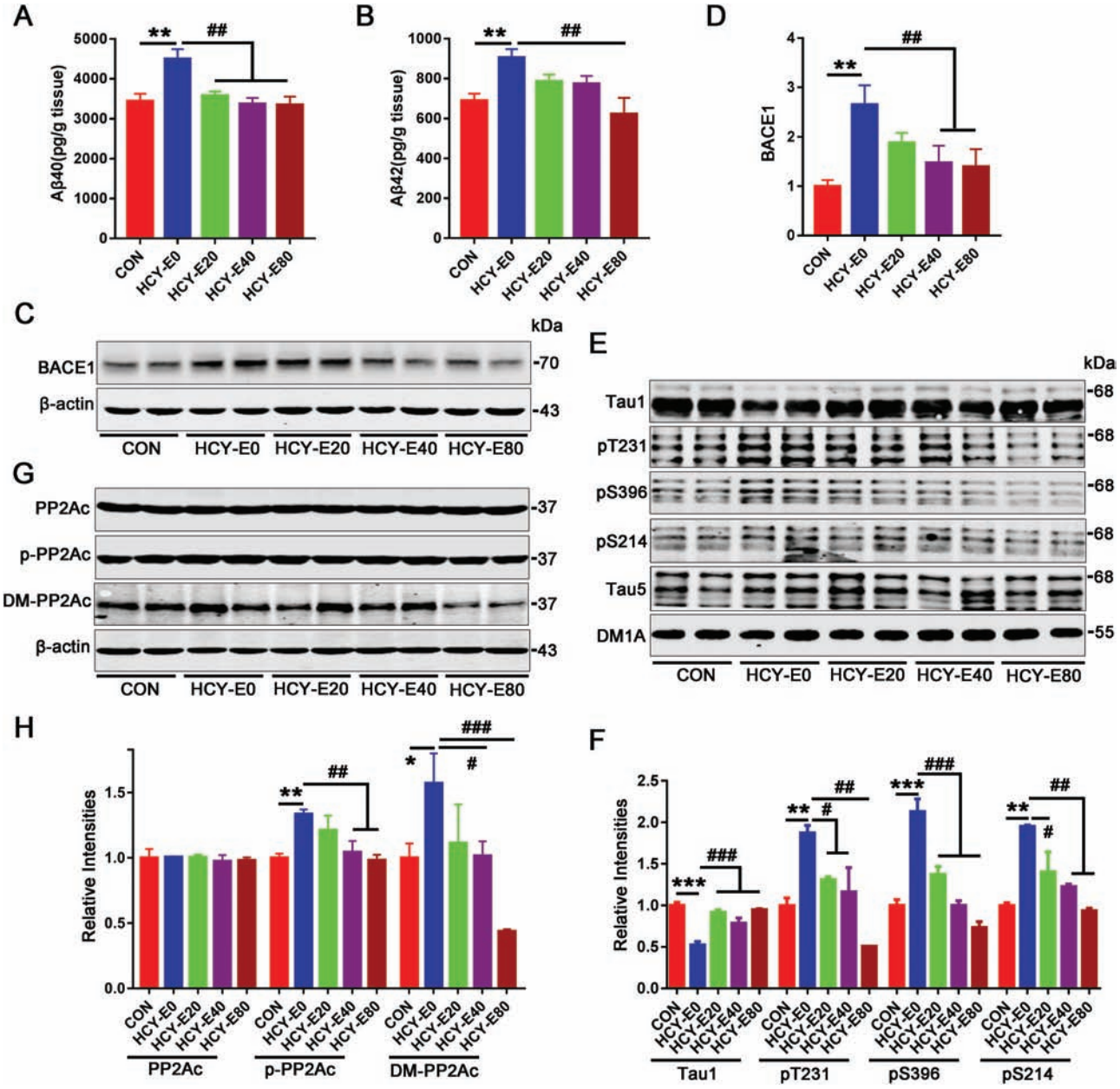

Figure 3. Emodin eliminated Aβ overproduction and tau hyperphosphorylation. Hippocampal Aβ40 (A) and Aβ42 (B) were detected by ELISA (pg/g tissue) (n = 6). Levels of β-site amyloid precursor protein-cleaving enzyme 1 (BACE1) (C–D), total tau (Tau5), tau unphosphorylation at Ser198/199/202 (Tau1) and tau phosphorylated at Thr231 (pT231), Ser396 (pS396) and Ser214 (pS214) (E–F) were measured by western blotting and quantitatively analyzed (n = 6). Levels of the catalytic subunit of protein phosphatase 2A (PP2Ac), its Tyr307-phosphorylation form (p-PP2Ac), and its demethylated form (DM-PP2Ac) (G–H) were measured by western blotting and quantitatively analyzed (n = 6). Data were expressed as the means ± SEM. $^{*}P < .05$, $^{**}P < .01$, $^{***}P < .001$ vs CON. $^{\#}P < .05$, $^{\#\#}P < .01$, $^{\#\#\#}P < .001$ vs HCY-E0.

Oxidative stress and DNA methylation impairments are included in HHcy-induced damages. Here, hippocampal levels of MDA [$F_{(4, 15)} = 3.568$, $P = .0309$] were significantly increased, and SOD1 levels [$F_{(4, 15)} = 4.339$, $P = .0157$] were decreased in HCY-E0 rats compared with the CON rats (Figure 4A–B). The increased MDA and decreased SOD1 levels were attenuated in the HCY-E40 and HCY-E80 rats (Figure 4A–B).

The hippocampal levels of DNA methyltransferases (DNMTs) were detected, and DNMT1 and DNMT3β, but not DNMT3α, were increased in the HCY-E0 rats. The levels of DNMT1 and DNMT3β in the HCY-E40 and HCY-E80 rats were significantly lower than in the HCY-E0 rats [$F_{(4, 25)} = 21.37$ for DNMT1, $P < .0001$; $F_{(4, 25)} = 0.5228$ for DNMT3α, $P = .7198$; $F_{(4, 25)} = 14.02$ for DNMT3β, $P < .0001$; Figure 4C–D].

Emodin Attenuated Damage of Cerebral Microvessels in HCY Rats

Cerebral vessels were visualized by the immunohistochemical staining of RECA-1 (an endothelial marker, Figure 5A–C), fluorescence of FITC (Figure 5D–E), and HE staining (Figure 5F). No differences were observed in the microvessel densities in the hippocampi and primary somatosensory cortex (S1Cx) of these 5 groups of rats (data not shown). However, in the RECA-1-imaged

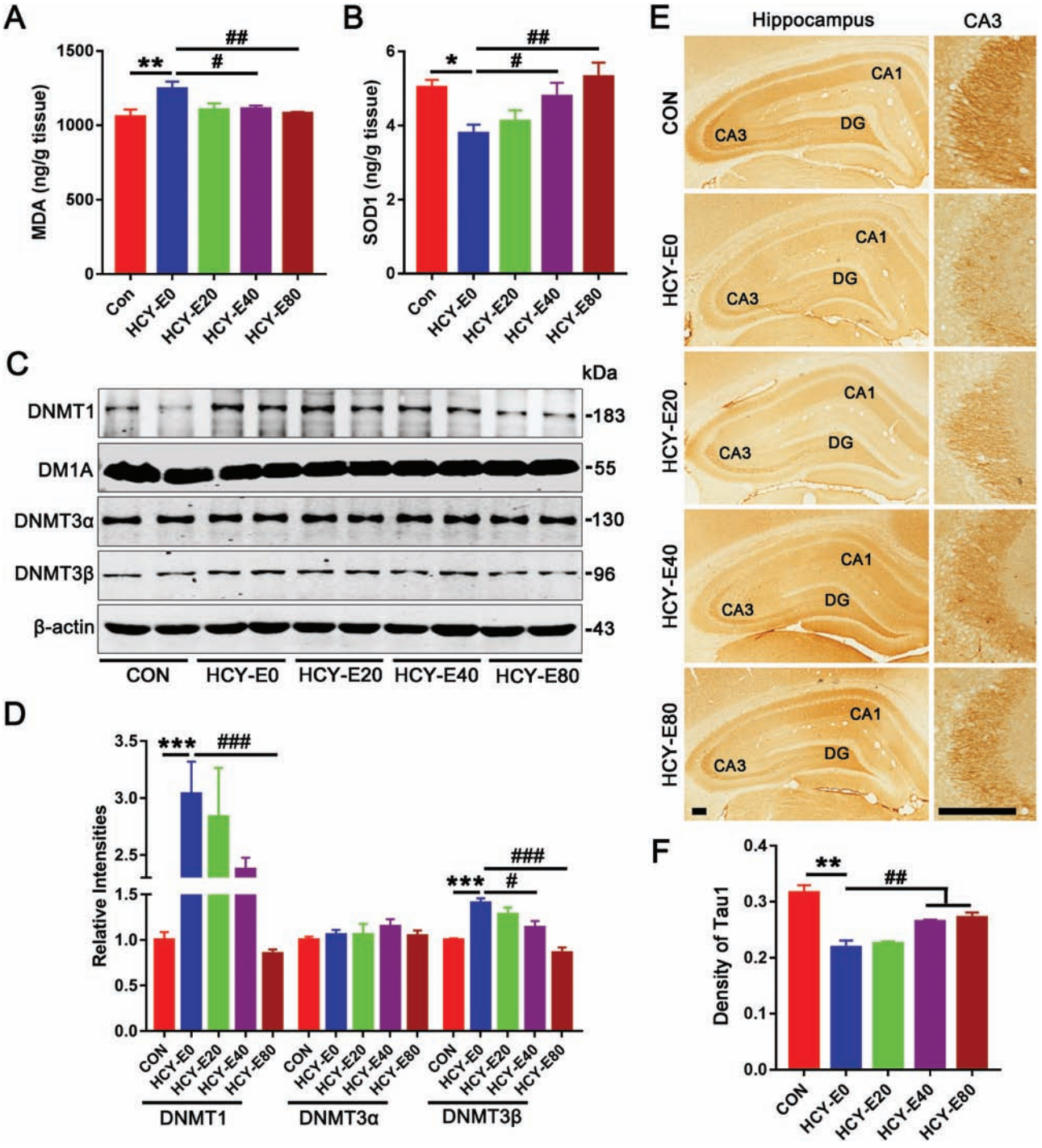

Figure 4. Emodin reversed hippocampal oxidative stress and upregulation of DNA methylation methyltransferases. Hippocampal malondialdehyde (MDA) (A) and superoxide dismutase 1 (SOD1) (B) were detected by ELISA (ng/g tissue) (n = 4). Levels of DNA methyltransferases (DNMTs), e.g., DNMT1, DNMT3α and DNMT3β (C–D), were measured by western blotting and quantitatively analyzed (n = 6). Hippocampi with Tau1-based immunohistochemical staining were shown (E), and the densities of Tau1 positive cells were quantitatively analyzed (F) (bar = 200 μm, n = 6). Data were expressed as the means ± SEM. $^{*}P < .05$, $^{**}P < .01$, $^{***}P < .001$ vs CON. $^{\#}P < .05$, $^{\#\#}P < .01$, $^{\#\#\#}P < .001$ vs HCY-E0.

vascular networks, we observed decreased lumen diameters of microarterioles by an intermittent dilatation manner both in the S1Cx (Figure 5B) and hippocampi (Figure 5C) of the HCY-E0 rats. Comparatively, the cerebral microvessels in the HCY-E80 rats presented normal morphological features similar to the CON rats (Figure 5B–C). Extravascular leakage of microvessels was assayed by FITC perfusion, which is a method of visualizing vasculature and extravascular leakage (Miyata and Morita, 2011). In the hippocampi and corpus callosum of the HCY-E0 rats, the green fluorescence of FITC was observed outside of the microvessels (Figure 5D). And in some hippocampal microvessels in the HCY-E0 rats, the bunchy exfoliated endothelial cells were clogged the vessels (Figure 5E, angiemphraxis). By HE staining, hyalinosis, increased perivascular space and splitting

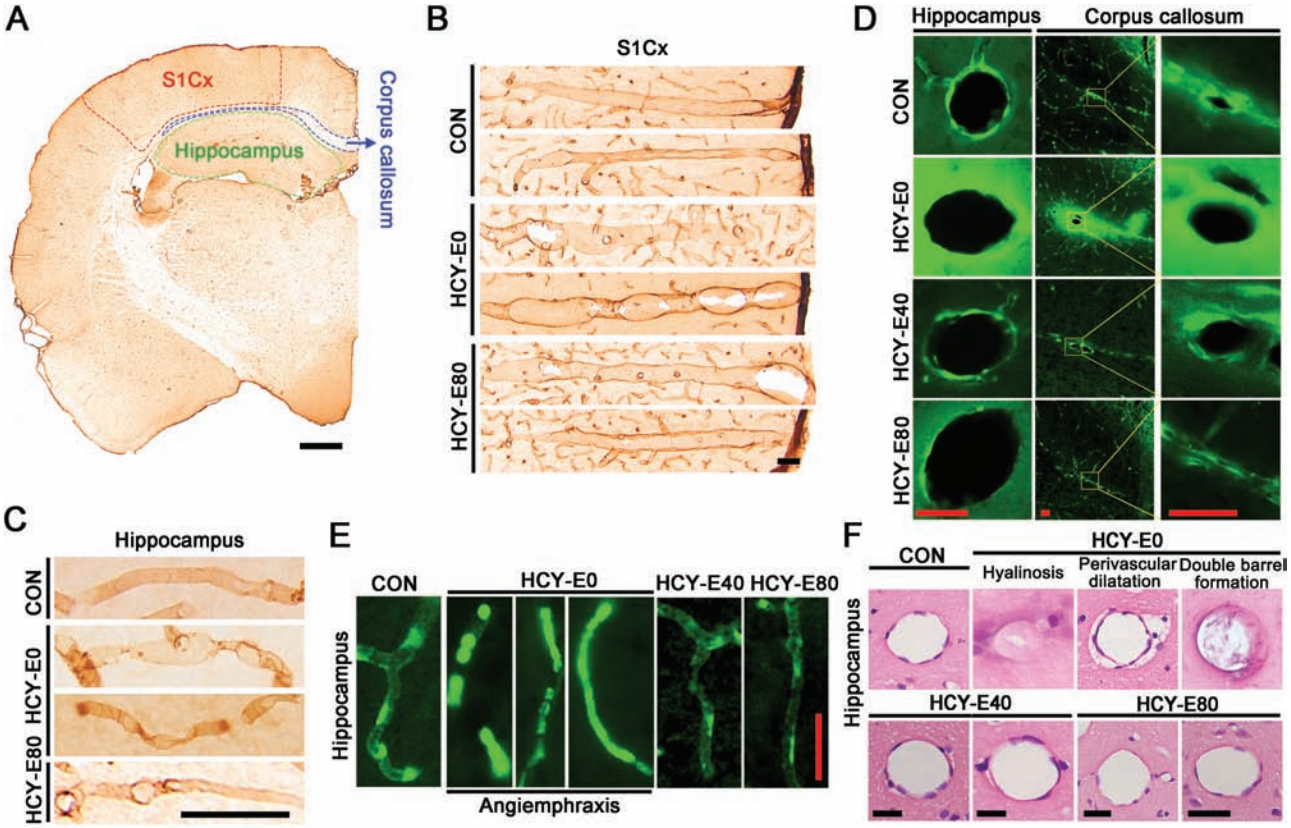

Figure 5. Morphological changes of cerebral microvessels. Cerebral vessels were visualized by immunohistochemical staining of RECA-1 (an endothelial marker, Figure 5A–C), the fluorescence of fluorescein isothiocyanate (FITC) (Figure 5D–E), and HE staining (Figure 5F). The locations of the hippocampi, primary somatosensory cortex (S1Cx), and corpus callosum were shown in A (bar = 1 mm). The decreased lumen diameters of microarterioles by an intermittent dilatation manner in the S1Cx (B) and hippocampi (C) were imaged by RECA-1-based immunohistochemical staining (bar = 50 μm). Extravascular leakage (D) and angiemphraxis (E) of microvessels were shown by the fluorescence of FITC (bar = 50 μm). The hyalinosis (1), increased perivascular space (perivascular dilatation, (2) and splitting of the walls (double barrel formation, (3) of microvessels were shown by HE is staining (F) (bar = 50 μm).

of the walls (double-barrel formation) were also detected in the hippocampi of the HCY-E0 rats (Figure 5F). However, extravascular leakage of FITC, angiemphraxis, hyalinosis, increased perivascular space, and splitting of the walls were not observed (Figure 5D–F) in the brains of the HCY-E40 and HCY-E80 rats.

Microglia Activation in the Hippocampi of HCY Rats Was Inhibited by Emodin

Increased solidity (the ratio between the positive area and the convex area) represents the activation of microglia (Soltys et al., 2001). By Iba1 (a microglial marker)-based immunohistochemical staining (Figure 6A), HCY-E0 rats had higher microglial solidities in both the hippocampi (0.26 ± 0.01) and S1Cx (0.24 ± 0.01), while the solidities in the HCY-E40 (hippocampi, 0.18 ± 0.01; S1Cx, 0.16 ± 0.01) and HCY-E80 rats (hippocampi, 0.17 ± 0.02; S1Cx, 0.15 ± 0.01) were lower [$F_{(4, 70)} = 20.34$ in the S1Cx, $P < .001$; $F_{(4, 70)} = 28.21$ in hippocampi, $P < .001$; Figure 6B–C].

The HCY-E0 rats had higher levels of IL-6 (4028 ± 55.7 pg/g tissue) and TNF-α (2609 ± 88.5 pg/g tissue) than the CON rats in hippocampi (IL-6, 3646 ± 50.3 pg/g tissue; TNF-α, 2085 ± 121.4 pg/g tissue), while both the HCY-E40 and HCY-E80 rats had lower levels of IL-6 and TNF-α [$F_{(4, 15)} = 6.023$ for IL-6, $P = .0043$; $F_{(4, 15)} = 4.503$ for TNF-α, $P = .0137$; Figure 6D–E]. The plasma levels of IL-6 and TNF-α showed no difference (data not shown). The hippocampal nuclear factor-κB p65 (NF-κB p65) was increased in the HCY-E0 rats (190.9% of CON rats), but not in the HCY-E40 and HCY-E80 rats [$F_{(4, 25)} = 16.36$, $P < .0001$; Figure 6F–G]. Further, 5-lipoxygenase (5-LO) levels in the HCY-E0 rats increased to approximately 220% of CON rats [$F_{(4, 25)} = 5.68$, $P = .0021$; Figure 6F, H], and this increase was confirmed by immunohistochemical staining (Figure 6I). The HCY-E40 and HCY-E80 rats had significantly lower 5-LO levels (Figure 6F, H, I). All these data suggested that HHcy-induced inflammation could be rescued by emodin treatment.

Discussion

Although there are reports of cognitive function improvements after high-dose Vit B therapy in individuals with cognition decline and elevated plasma Hcy levels (Nilsson et al., 2001; Durga et al., 2007; de Jager et al., 2012), 3 randomized controlled trials found no effects of vitamin supplementation on cognitive tests (Aisen et al., 2008; Kwok et al., 2011; Köbe et al., 2016). Several other trials in elders with vascular disease (Stott et al., 2005) and individuals with mild cognitive impairment (van Uffelen et al., 2008) and dementia (Sommer et al., 2003) also showed that Vit B treatment did not improve cognition despite lowering Hcy. Furthermore, some meta-analyses suggest that folate and Vit B supplementation do not provide any significant advantage in slowing down or preventing the progression of cognitive decline (Ford and Almeida, 2012; van der Zwaluw et al., 2014; Smith et al., 2015; Zhang et al., 2017). Therefore, reducing Hcy levels is not sufficient to improve HHcy-induced cognitive impairments. Emodin is a bioactive anthraquinone present in

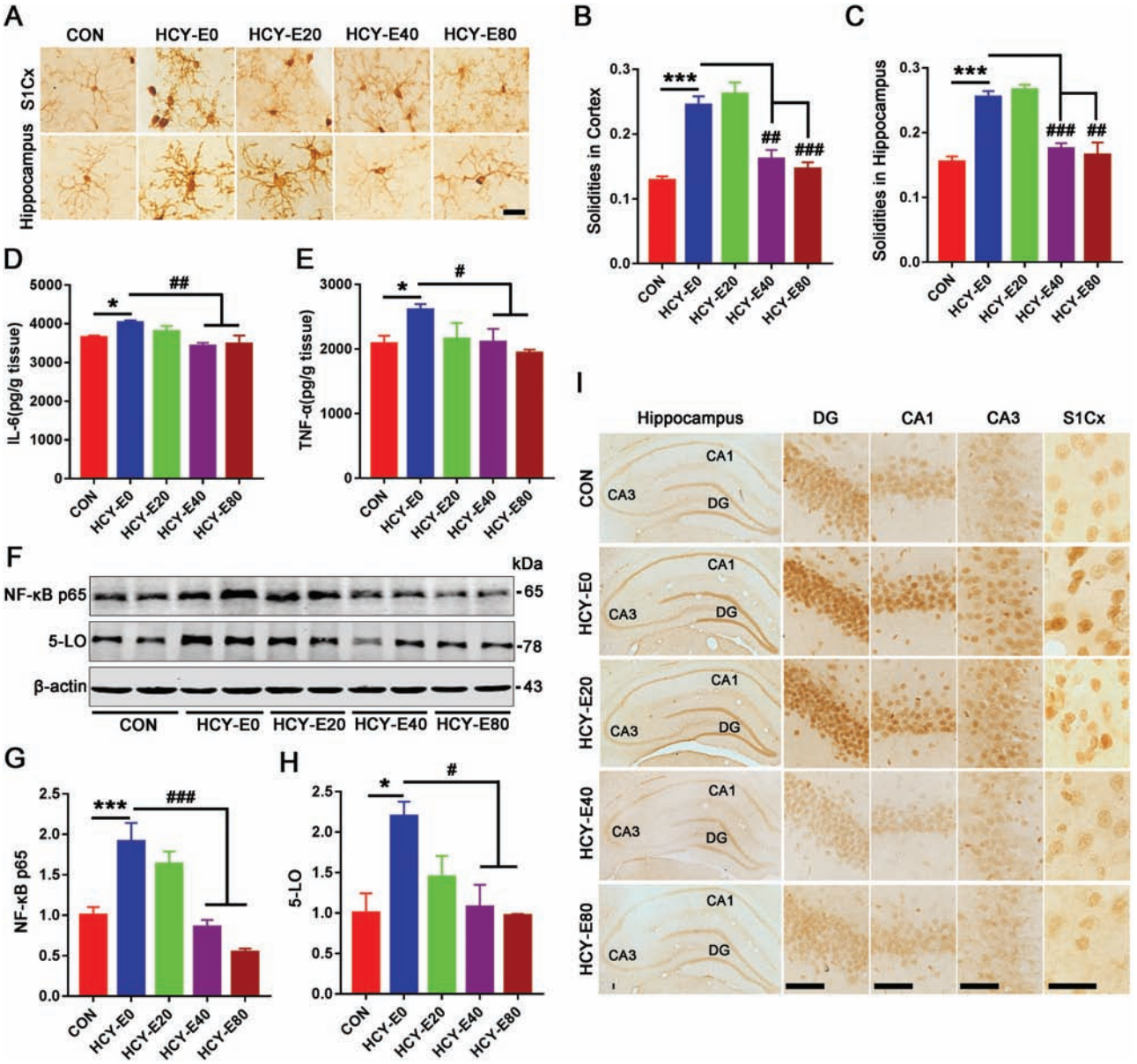

Figure 6. Microglia activation and inflammation in HCY rats was inhibited by emodin. Microglia in the hippocampi and S1Cx were shown by immunohistochemical staining with Iba1, a marker of microglia (A, bar = 25 μm). The solidities of microglia in the S1Cx (B) and hippocampi (C) were calculated to assess the activation of microglia (n = 6). Levels of IL-6 (D) and TNF-α (E) in the hippocampi were detected (pg/g tissue, n = 4) by ELISA. Levels of NF-κB p65 and 5-lipoxygenase (5-LO) in the hippocampi were measured by western blotting (F, n = 6) and quantitatively analyzed (G–H). Hippocampi and S1Cx with 5-LO-based immunohistochemical staining were shown in (I) (bar = 25 μm). Data were expressed as the means ± SEM. $^{*}P < .05$, $^{***}P < .001$ vs CON. $^{\#}P < .05$, $^{\#\#}P < .01$, $^{\#\#\#}P < .001$ vs HCY-E0.

some prescriptions of traditional Chinese medicine with cerebral protections. Here, although plasma Hcy levels did not decrease, the emodin-treated HHcy rats had better behavioral performances. And in the hippocampi of emodin-treated HHcy rats, the neuron loss in the CA3 region, the decreased synapse-related proteins including synaptophysin, synapsin 1 and NR1, and the reduced phosphorylated CREB at Ser133 were remedied by emodin.

Cerebral hypoperfusion is a risk factor for cognitive impairments (Park et al., 2014; Garcia-Bonilla et al., 2015; Faraco et al., 2016). HHcy was reported to impair cerebrovascular endothelial function and interfere with nitric oxide-mediated cerebral blood flow (Woo et al., 1997; Bang et al., 2016). In the CBS-knockout mouse (an HHcy model), HHcy was shown to increase brain permeability (Tyagi et al., 2012). A study on a mouse model produced by feeding with food containing excess methionine and deficits in folate, Vit B6, and Vit B12 reported that HHcy was associated with increased microhemorrhages in the brain (Sudduth et al., 2013). Hcy level was regarded as the marker of endothelial function not only in macroangiopathy but also clinically in cerebral microangiopathy (Bang et al., 2016). And HHcy was claimed more closely associated with small vessel disease than large vessel disease (Feng et al., 2013). In this study, HHcy induced several microangiopathic alterations including intermittent increased lumen diameter, extravascular leakage, hyalinosis, increased perivascular space, and splitting of the walls, all of which contribute to cerebral hypoperfusion (Kalaria, 2016). Emodin significantly ameliorated HHcy-induced

microangiopathic alterations, suggesting its role in improving cerebral perfusion.

Besides cerebral hypoperfusion, HHcy induces Aβ accumulation, tau hyperphosphorylation, and cognition impairments in AD models and normal animals (Fuso et al., 2008; Troen et al., 2008a, 2008b; Zhang et al., 2009; Fuso et al., 2012; Nicolia et al., 2010; Chai et al., 2013; Li et al., 2014). We reported that HHcy enhanced the phosphorylation of amyloid precursor protein at Thr688 by inhibiting PP2A and thus increased Aβ production in vivo (Zhang et al., 2009). BACE1 is the rate-limiting enzyme for Aβ production. Levels of BACE1 and Aβ were reported upregulated in Vit B deficiency mice with HHcy (Fuso et al., 2008). Here, the increased BACE1 was also detected in the hippocampi of HCY-E0 rats, suggesting its potential role in HHcy-induced Aβ overproduction. The density of neurofibrillary tangles containing hyperphosphorylated tau, which could be dephosphorylated by PP2A, correlates with dementia of AD (Tian and Wang, 2002). HHcy was reported to increase tau phosphorylation by inhibiting PP2A in vivo (Zhang et al., 2008). Previous studies showed that the anthraquinone family (including emodin) inhibited tau aggregation in vitro (Pickhardt et al., 2005). In this research, emodin opposed HHcy-induced inhibition of PP2A in vivo and thus attenuated HHcy-induced tau hyperphosphorylation and Aβ overproduction.

PP2A, a serine/threonine protein phosphatase, exists predominantly as heterotrimers containing a 65-kDa subunit A ($PP2A_A$) acting as a scalfold for the association of a 36-kDa $PP2A_C$, one of a variety of regulatory subunits ($PP2A_B$), and $PP2A_C$. The highly conserved carboxyl-terminal sequence of $PP2A_C$ has a Thr-Pro-Asp-Tyr-Phe-Leu motif, which contains both the site of phosphrylation (Tyr307) and the site (Leu309) of a reversible methylesterification (Tolstykh et al., 2000; Janssens and Goris, 2001). The methylation at Leu309, which is specifically catalyzed by methylesterase (PME) and methyltransferase, promotes the binding of $PP2A_B$ to the core enzyme and thus increases the activity of PP2A. We have shown that HHcy increased PME levels and thereby induced the demethylation and inhibition of $PP2A_C$ (Zhang et al., 2008). Thus, emodin probably decreased the demethylation of $PP2A_C$ in this study by restoring the HHcy-induced elevation of PME.

DNA methylation regulated by DNMTs and DNA demethylases is an epigenetic process in gene regulation. DNMTs are detected in the adult brain and important in synaptic plasticity (Feng et al., 2005, 2010; Levenson et al., 2006; Miller and Sweatt, 2007; LaPlant et al., 2010). It was reported that HHcy increased DNMT1 mRNA and protein levels in monocyte-derived foam cells (Liang et al., 2013) and human umbilical vein endothelial cells (Zhang et al., 2013). Feeding a folate/methyl-deficient diet caused global DNA hypermethylation with increased DNMT3α in the brains of Fisher 344 rats (Pogribny et al., 2008). A previous study showed the increased DNA methylation with increased DNMT1 and DNMT3α protein levels in HHcy mice brain (Kalani et al., 2014). However, HHcy was also associated with the downregulated DNMTs both in vitro (Lin et al., 2014; Ma et al., 2017) and in vivo (Fuso et al., 2011; Li et al., 2017). Diet and genetically induced HHcy in 3×Tg AD mice resulted a significant increase of the S-adenosylhomocysteine/S-adenosylmethionine ratio, reduced DNMTs (DNMT1, DNMT3α, and DNMT3β), and hypomethylation of 5-LO DNA in the brain cortex homogenates (Li et al., 2017).

In addition to the well-known function in catalyzing methylation, DNMT1, DNMT3α, and DNMT3β were reported have DNA demethylating activities (Chen et al., 2012, 2013). Thus, although the HHcy induced the increased hippocampal DNMT1 and DNMT3β in this research, more in-depth research is needed to reveal the relationship between HHcy and DNMTs activities. A demethylating drug, 5-aza-2'-deoxycytidine, specifically demethylated 2 CpG sites at positions +298 and +351 in the 5'-untranslated region of the BACE1 gene and thus increased both the mRNA and protein levels of BACE1 in a dose-dependent manner in BV-2 microglial cells (Byun et al., 2012), suggesting the gene expression of BACE1 might be upregulated by DNA demethylation. Accordingly, although HHcy-increased BACE1, DNMT1, and DNMT3β levels were observed in this study, whether the increased BACE1 is due to DNA demethylation activated by the increased DNMTs needs further studies. The reduction of DNMT1 in heterozygous null mice conferred protection against stroke (Endres et al., 2000), and reduction of DNMT3α decreased the apoptosis of NSC34 cells (Chestnut et al., 2011). Here, emodin-treated HCY rats with reduced hippocampal DNMT1 and DNMT3β had better behavioral scores. These data suggested that downregulating DNMTs is important in antagonizing brain injuries. Additionally, emodin exerts its antitumor activity by regulating the levels of DNMTs. In Panc-1 cells, emodin decreased the methylation levels in the promoter region of several key tumor-suppressor genes by inhibiting the expression of DNMT1 and DNMT3α (Pan et al., 2016). However, in lymphoma Raji cells, emodin inhibited cell proliferation potentially by increasing DNMT3α (Lin et al., 2017). Besides the protein levels, the activities of DNMTs are influenced by several other factors, including local chromatin microenvironments (van der Wijst et al., 2015). Thus, emodin might exert different effects on DNMTs in different pathological conditions.

Inflammation is a potential mediator of cognitive deficits in AD (Serpente et al., 2014). Microglia with different morphological types are key players of cerebral inflammation, and this microglia engaged in inflammation is a major source of reactive oxygen species (Soltys et al., 2001; Block and Hong, 2007). Activated microglia release a series of proinflammatory mediators including cytokines, complement components, and free radicals, all of which potentially contribute to oxidative stress and eventually trigger neuronal dysfunction and death, synapse loss, and cognitive impairments (Chinnici et al., 2007; Hong et al., 2016). 5-LO, an inflammatory enzyme widely expressed in the brain, plays a key role in brain damage and increases with aging (Bessis et al., 2007). Pharmacologic inhibition of 5-LO improves memory, rescues neuroinflammation and synaptic dysfunction, and ameliorates tau pathology in a transgenic model of tauopathy (Chu et al., 2012). NF-κB is a master regulator of inflammation and also a sensor of oxidative stress. Activating NF-κB induce some cytotoxic factors that exacerbate inflammation and oxidative stress and promote apoptosis (Pahl, 1999), suggesting its prominent strategic position in oxidative stress and inflammation. In this study, HHcy-induced cerebral inflammation—characterized by activated microglia, increased levels of 5-LO, NF-κB p65, TNF-α, and IL-6 and activated oxidative stress—was rescued by emodin. However, the plasma TNF-α and IL-6 levels were not affected by HHcy, indicating the possibility that cerebral inflammation may occur very early after HHcy treatment.

Here, HHcy rats developed obvious cognitive deficits with several AD-like features in the brain, including Aβ overproduction, tau hyperphosphorylation, loss of neurons and synapses, inflammation, and abnormal microangiopathic alterations. Emodin effectively improved the cognitive deficits and rescued the AD-like features induced by HHcy, although it did not reduce the plasma Hcy level. Thus, emodin represents a novel potential candidate agent for HHcy-induced cognitive deficits.

Acknowledgments

This work was supported by grants from the Natural Science Foundation of China (91539112) and Integrated Innovative Team for Major Human Diseases Program of Tongji Medical College.

Statement of Interest

None.

References

Aisen PS, Schneider LS, Sano M, Diaz-Arrastia R, van Dyck CH, Weiner MF, Bottiglieri T, Jin S, Stokes KT, Thomas RG, Thal LJ, Alzheimer Disease Cooperative Study (2008) High-dose B vitamin supplementation and cognitive decline in alzheimer disease: a randomized controlled trial. Jama 300:1774–1783.

Bang OY, Chung JW, Ryoo S, Moon GJ, Kim GM, Chung CS, Lee KH (2016) Brain microangiopathy and macroangiopathy share common risk factors and biomarkers. Atherosclerosis 246:71–77.

Bessis A, Béchade C, Bernard D, Roumier A (2007) Microglial control of neuronal death and synaptic properties. Glia 55:233–238.

Block ML, Hong JS (2007) Chronic microglial activation and progressive dopaminergic neurotoxicity. Biochem Soc Trans 35:1127–1132.

Broadbent NJ, Gaskin S, Squire LR, Clark RE (2010) Object recognition memory and the rodent hippocampus. Learn Mem 17:5–11.

Byun CJ, Seo J, Jo SA, Park YJ, Klug M, Rehli M, Park MH, Jo I (2012) DNA methylation of the 5'-untranslated region at +298 and +351 represses BACE1 expression in mouse BV-2 microglial cells. Biochem Biophys Res Commun 417:387–392.

Chai GS, Jiang X, Ni ZF, Ma ZW, Xie AJ, Cheng XS, Wang Q, Wang JZ, Liu GP (2013) Betaine attenuates alzheimer-like pathological changes and memory deficits induced by homocysteine. J Neurochem 124:388–396.

Chen CC, Wang KY, Shen CK (2012) The mammalian de novo DNA methyltransferases DNMT3A and DNMT3B are also DNA 5-hydroxymethylcytosine dehydroxymethylases. J Biol Chem 287:33116–33121.

Chen CC, Wang KY, Shen CK (2013) DNA 5-methylcytosine demethylation activities of the mammalian DNA methyltransferases. J Biol Chem 288:9084–9091.

Chestnut BA, Chang Q, Price A, Lesuisse C, Wong M, Martin LJ (2011) Epigenetic regulation of motor neuron cell death through DNA methylation. J Neurosci 31:16619–16636.

Chinnici CM, Yao Y, Praticò D (2007) The 5-lipoxygenase enzymatic pathway in the mouse brain: young versus old. Neurobiol Aging 28:1457–1462.

Chu J, Giannopoulos PF, Ceballos-Diaz C, Golde TE, Praticò D (2012) 5-lipoxygenase gene transfer worsens memory, amyloid, and tau brain pathologies in a mouse model of alzheimer disease. Ann Neurol 72:442–454.

Clarke R, Harrison G, Richards S, Vital Trial Collaborative Group (2003) Effect of vitamins and aspirin on markers of platelet activation, oxidative stress and homocysteine in people at high risk of dementia. J Intern Med 254:67–75.

Cotter AM, Molloy AM, Scott JM, Daly SF (2003) Elevated plasma homocysteine in early pregnancy: a risk factor for the development of nonsevere preeclampsia. Am J Obstet Gynecol 189:391–394.

de Jager CA, Oulhaj A, Jacoby R, Refsum H, Smith AD (2012) Cognitive and clinical outcomes of homocysteine-lowering B-vitamin treatment in mild cognitive impairment: a randomized controlled trial. Int J Geriatr Psychiatry 27:592–600.

de Koning EJ, van der Zwaluw NL, van Wijngaarden JP, Sohl E, Brouwer-Brolsma EM, van Marwijk HW, Enneman AW, Swart KM, van Dijk SC, Ham AC, van der Velde N, Uitterlinden AG, Penninx BW, Elders PJ, Lips P, Dhonukshe-Rutten RA, van Schoor NM, de Groot LC (2016) Effects of two-year vitamin B12 and folic acid supplementation on depressive symptoms and quality of life in older adults with elevated homocysteine concentrations: additional results from the B-PROOF study, an RCT. Nutrients 8:pii: E748.

Desouza C, Keebler M, McNamara DB, Fonseca V (2002) Drugs affecting homocysteine metabolism: impact on cardiovascular risk. Drugs 62:605–616.

Durga J, van Boxtel MP, Schouten EG, Kok FJ, Jolles J, Katan MB, Verhoef P (2007) Effect of 3-year folic acid supplementation on cognitive function in older adults in the FACIT trial: a randomised, double blind, controlled trial. Lancet 369:208–216.

Endres M, Meisel A, Biniszkiewicz D, Namura S, Prass K, Ruscher K, Lipski A, Jaenisch R, Moskowitz MA, Dirnagl U (2000) DNA methyltransferase contributes to delayed ischemic brain injury. J Neurosci 20:3175–3181.

Faraco G, Sugiyama Y, Lane D, Garcia-Bonilla L, Chang H, Santisteban MM, Racchumi G, Murphy M, Van Rooijen N, Anrather J, Iadecola C (2016) Perivascular macrophages mediate the neurovascular and cognitive dysfunction associated with hypertension. J Clin Invest 126:4674–4689.

Feng C, Bai X, Xu Y, Hua T, Huang J, Liu XY (2013) Hyperhomocysteinemia associates with small vessel disease more closely than large vessel disease. Int J Med Sci 10:408–412.

Feng J, Chang H, Li E, Fan G (2005) Dynamic expression of de novo DNA methyltransferases dnmt3a and dnmt3b in the central nervous system. J Neurosci Res 79:734–746.

Feng J, Zhou Y, Campbell SL, Le T, Li E, Sweatt JD, Silva AJ, Fan G (2010) Dnmt1 and dnmt3a maintain DNA methylation and regulate synaptic function in adult forebrain neurons. Nat Neurosci 13:423–430.

Fioravanti M, Ferrario E, Massaia M, Cappa G, Rivolta G, Grossi E, Buckley AE (1998) Low folate levels in the cognitive decline of elderly patients and the efficacy of folate as a treatment for improving memory deficits. Arch Gerontol Geriatr 26:1–13.

Finkelstein JD (1998) The metabolism of homocysteine: pathways and regulation. Eur J Pediatr 157:S40–S44.

Ford AH, Almeida OP (2012) Effect of homocysteine lowering treatment on cognitive function: a systematic review and meta-analysis of randomized controlled trials. J Alzheimers Dis 29:133–149.

Fuso A, Nicolia V, Cavallaro RA, Ricceri L, D'Anselmi F, Coluccia P, Calamandrei G, Scarpa S (2008) B-vitamin deprivation induces hyperhomocysteinemia and brain S-adenosylhomocysteine, depletes brain S-adenosylmethionine, and enhances PS1 and BACE expression and amyloid-beta deposition in mice. Mol Cell Neurosci 37:731–746.

Fuso A, Nicolia V, Cavallaro RA, Scarpa S (2011) DNA methylase and demethylase activities are modulated by one-carbon metabolism in Alzheimer's disease models. J Nutr Biochem 22:242–251.

Fuso A, Nicolia V, Ricceri L, Cavallaro RA, Isopi E, Mangia F, Fiorenza MT, Scarpa S (2012) S-adenosylmethionine reduces the progress of the alzheimer-like features induced by

B-vitamin deficiency in mice. Neurobiol Aging 33:1482.e1–1482.16.

Garcia-Bonilla L, Racchumi G, Murphy M, Anrather J, Iadecola C (2015) Endothelial CD36 contributes to postischemic brain injury by promoting neutrophil activation via CSF3. J Neurosci 35:14783–14793.

Gong H, Tang W, Wang H, Xia Q, Huang X (2011) Effects of food and gender on the pharmacokinetics of rhein and emodin in rats after oral dosing with da-cheng-qi decoction. Phytother Res 25:74–80.

Hong S, Beja-Glasser VF, Nfonoyim BM, Frouin A, Li S, Ramakrishnan S, Merry KM, Shi Q, Rosenthal A, Barres BA, Lemere CA, Selkoe DJ, Stevens B (2016) Complement and microglia mediate early synapse loss in alzheimer mouse models. Science 352:712–716.

Huang HC, Chu SH, Chao PD (1991) Vasorelaxants from chinese herbs, emodin and scoparone, possess immunosuppressive properties. Eur J Pharmacol 198:211–213.

Janssens V, Goris J (2001) Protein phosphatase 2A: a highly regulated family of serine/threonine phosphatases implicated in cell growth and signalling. Biochem J 353:417–439.

Kalani A, Kamat PK, Givvimani S, Brown K, Metreveli N, Tyagi SC, Tyagi N (2014) Nutri-epigenetics ameliorates blood-brain barrier damage and neurodegeneration in hyperhomocysteinemia: role of folic acid. J Mol Neurosci 52:202–215.

Kalaria RN (2016) Neuropathological diagnosis of vascular cognitive impairment and vascular dementia with implications for Alzheimer's disease. Acta Neuropathol 131:659–685.

Kamat PK, Vacek JC, Kalani A, Tyagi N (2015) Homocysteine induced cerebrovascular dysfunction: a link to Alzheimer's disease etiology. Open Neurol J 9:9–14.

Kitzlerová E, Fisar Z, Jirák R, Zvěrová M, Hroudová J, Benaková H, Raboch J (2014) Plasma homocysteine in alzheimer's disease with or without co-morbid depressive symptoms. Neuro Endocrinol Lett 35:42–49.

Köbe T, Witte AV, Schnelle A, Lesemann A, Fabian S, Tesky VA, Pantel J, Flöel A (2016) Combined omega-3 fatty acids, aerobic exercise and cognitive stimulation prevents decline in gray matter volume of the frontal, parietal and cingulate cortex in patients with mild cognitive impairment. Neuroimage 131:226–238.

Kumar A, Palfrey HA, Pathak R, Kadowitz PJ, Gettys TW, Murthy SN (2017) The metabolism and significance of homocysteine in nutrition and health. Nutr Metab (Lond) 14:78.

Kumar M, Goudihalli S, Mukherjee K, Dhandapani S, Sandhir R (2018) Methylenetetrahydrofolate reductase C677T variant and hyperhomocysteinemia in subarachnoid hemorrhage patients from India. Metab Brain Dis. Epub ahead of print.2018 Jun 21. doi: 10.1007/s11011-018-0268-5.

Kwok T, Lee J, Law CB, Pan PC, Yung CY, Choi KC, Lam LC (2011) A randomized placebo-controlled trial of homocysteine lowering to reduce cognitive decline in older demented people. Clin Nutr 30:297–302.

LaPlant Q, et al. (2010) Dnmt3a regulates emotional behavior and spine plasticity in the nucleus accumbens. Nat Neurosci 13:1137–1143.

Levenson JM, Roth TL, Lubin FD, Miller CA, Huang IC, Desai P, Malone LM, Sweatt JD (2006) Evidence that DNA (cytosine-5) methyltransferase regulates synaptic plasticity in the hippocampus. J Biol Chem 281:15763–15773.

Li JG, Chu J, Barrero C, Merali S, Praticò D (2014) Homocysteine exacerbates β-amyloid pathology, tau pathology, and cognitive deficit in a mouse model of alzheimer disease with plaques and tangles. Ann Neurol 75:851–863.

Li JG, Barrero C, Gupta S, Kruger WD, Merali S, Praticò D (2017) Homocysteine modulates 5-lipoxygenase expression level via DNA methylation. Aging Cell 16:273–280.

Liang Y, Yang X, Ma L, Cai X, Wang L, Yang C, Li G, Zhang M, Sun W, Jiang Y (2013) Homocysteine-mediated cholesterol efflux via ABCA1 and ACAT1 DNA methylation in THP-1 monocyte-derived foam cells. Acta Biochim Biophys Sin (Shanghai) 45:220–228.

Lin N, Qin S, Luo S, Cui S, Huang G, Zhang X (2014) Homocysteine induces cytotoxicity and proliferation inhibition in neural stem cells via DNA methylation in vitro. Febs J 281:2088–2096.

Lin Y, Chen W, Wang Z, Cai P (2017) Emodin promotes the arrest of human lymphoma raji cell proliferation through the UHRF1-DNMT3A-Δnp73 pathways. Mol Med Rep 16:6544–6551.

Ma SC, Hao YJ, Jiao Y, Wang YH, Xu LB, Mao CY, Yang XL, Yang AN, Tian J, Zhang MH, Jin SJ, Xu H, Jiang YD, Zhang HP (2017) Homocysteine-induced oxidative stress through TLR4/NF-κb/DNMT1-mediated LOX-1 DNA methylation in endothelial cells. Mol Med Rep 16:9181–9188.

Malouf M, Grimley EJ, Areosa SA (2003) Folic acid with or without vitamin B12 for cognition and dementia. Cochrane Database Syst Rev 2003:CD004514.

Miller CA, Sweatt JD (2007) Covalent modification of DNA regulates memory formation. Neuron 53:857–869.

Miyata S, Morita S (2011) A new method for visualization of endothelial cells and extravascular leakage in adult mouse brain using fluorescein isothiocyanate. J Neurosci Methods 202:9–16.

Morris R (1984) Developments of a water-maze procedure for studying spatial learning in the rat. J Neurosci Methods 11:47–60.

Nicolia V, Fuso A, Cavallaro RA, Di Luzio A, Scarpa S (2010) B vitamin deficiency promotes tau phosphorylation through regulation of GSK3BETA and PP2A. J Alzheimers Dis 19:895–907.

Nilsson K, Gustafson L, Hultberg B (2001) Improvement of cognitive functions after cobalamin/folate supplementation in elderly patients with dementia and elevated plasma homocysteine. Int J Geriatr Psychiatry 16:609–614.

Obeid R, McCaddon A, Herrmann W (2007) The role of hyperhomocysteinemia and B-vitamin deficiency in neurological and psychiatric diseases. Clin Chem Lab Med 45:1590–1606.

Pahl HL (1999) Activators and target genes of rel/NF-kappab transcription factors. Oncogene 18:6853–6866.

Pan FP, Zhou HK, Bu HQ, Chen ZQ, Zhang H, Xu LP, Tang J, Yu QJ, Chu YQ, Pan J, Fei Y, Lin SZ, Liu DL, Chen L (2016) Emodin enhances the demethylation by 5-aza-cdr of pancreatic cancer cell tumor-suppressor genes P16, RASSF1A and ppenk. Oncol Rep 35:1941–1949.

Park L, Wang G, Moore J, Girouard H, Zhou P, Anrather J, Iadecola C (2014) The key role of transient receptor potential melastatin-2 channels in amyloid-β-induced neurovascular dysfunction. Nat Commun 5:5318.

Pickhardt M, Gazova Z, von Bergen M, Khlistunova I, Wang Y, Hascher A, Mandelkow EM, Biernat J, Mandelkow E (2005) Anthraquinones inhibit tau aggregation and dissolve Alzheimer's paired helical filaments in vitro and in cells. J Biol Chem 280:3628–3635.

Pogribny IP, Karpf AR, James SR, Melnyk S, Han T, Tryndyak VP (2008) Epigenetic alterations in the brains of fisher 344 rats induced by long-term administration of folate/methyl-deficient diet. Brain Res 1237:25–34.

Prudova A, Bauman Z, Braun A, Vitvitsky V, Lu SC, Banerjee R (2006) S-adenosylmethionine stabilizes cystathionine

beta-synthase and modulates redox capacity. Proc Natl Acad Sci U S A 103:6489–6494.

Selhub J (1999) Homocysteine metabolism. Annu Rev Nutr 19:217–246.

Serpente M, Bonsi R, Scarpini E, Galimberti D (2014) Innate immune system and inflammation in Alzheimer's disease: from pathogenesis to treatment. Neuroimmunomodulation 21:79–87.

Sharma M, Tiwari M, Tiwari RK (2015) Hyperhomocysteinemia: impact on neurodegenerative diseases. Basic Clin Pharmacol Toxicol 117:287–296.

Shaywitz AJ, Greenberg ME (1999) CREB: a stimulus-induced transcription factor activated by a diverse array of extracellular signals. Annu Rev Biochem 68:821–861.

Smith AD, de Jager CA, Refsum H, Rosenberg IH (2015) Homocysteine lowering, B vitamins, and cognitive aging. Am J Clin Nutr 101:415–416.

Soltys Z, Ziaja M, Pawlínski R, Setkowicz Z, Janeczko K (2001) Morphology of reactive microglia in the injured cerebral cortex. Fractal analysis and complementary quantitative methods. J Neurosci Res 63:90–97.

Sommer BR, Hoff AL, Costa M (2003) Folic acid supplementation in dementia: a preliminary report. J Geriatr Psychiatry Neurol 16:156–159.

Srinivas G, Babykutty S, Sathiadevan PP, Srinivas P (2007) Molecular mechanism of emodin action: transition from laxative ingredient to an antitumor agent. Med Res Rev 27:591–608.

Stott DJ, MacIntosh G, Lowe GD, Rumley A, McMahon AD, Langhorne P, Tait RC, O'Reilly DS, Spilg EG, MacDonald JB, MacFarlane PW, Westendorp RG (2005) Randomized controlled trial of homocysteine-lowering vitamin treatment in elderly patients with vascular disease. Am J Clin Nutr 82:1320–1326.

Sudduth TL, Powell DK, Smith CD, Greenstein A, Wilcock DM (2013) Induction of hyperhomocysteinemia models vascular dementia by induction of cerebral microhemorrhages and neuroinflammation. J Cereb Blood Flow Metab 33:708–715.

Tian Q, Wang J (2002) Role of serine/threonine protein phosphatase in alzheimer's disease. Neurosignals 11:262–269.

Tolstykh T, Lee J, Vafai S, Stock JB (2000) Carboxyl methylation regulates phosphoprotein phosphatase 2A by controlling the association of regulatory B subunits. Embo J 19:5682–5691.

Troen AM (2005) The central nervous system in animal models of hyperhomocysteinemia. Prog Neuropsychopharmacol Biol Psychiatry 29:1140–1151.

Troen AM, Chao WH, Crivello NA, D'Anci KE, Shukitt-Hale B, Smith DE, Selhub J, Rosenberg IH (2008a) Cognitive impairment in folate-deficient rats corresponds to depleted brain phosphatidylcholine and is prevented by dietary methionine without lowering plasma homocysteine. J Nutr 138:2502–2509.

Troen AM, Shea-Budgell M, Shukitt-Hale B, Smith DE, Selhub J, Rosenberg IH (2008b) B-vitamin deficiency causes hyperhomocysteinemia and vascular cognitive impairment in mice. Proc Natl Acad Sci U S A 105:12474–12479.

Tyagi N, Qipshidze N, Munjal C, Vacek JC, Metreveli N, Givvimani S, Tyagi SC (2012) Tetrahydrocurcumin ameliorates homocysteinylated cytochrome-c mediated autophagy in hyperhomocysteinemia mice after cerebral ischemia. J Mol Neurosci 47:128–138.

van der Wijst MG, Venkiteswaran M, Chen H, Xu GL, Plösch T, Rots MG (2015) Local chromatin microenvironment determines DNMT activity: from DNA methyltransferase to DNA demethylase or DNA dehydroxymethylase. Epigenetics 10:671–676.

van der Zwaluw NL, Dhonukshe-Rutten RA, van Wijngaarden JP, Brouwer-Brolsma EM, van de Rest O, In 't Veld PH, Enneman AW, van Dijk SC, Ham AC, Swart KM, van der Velde N, van Schoor NM, van der Cammen TJ, Uitterlinden AG, Lips P, Kessels RP, de Groot LC (2014) Results of 2-year vitamin B treatment on cognitive performance: secondary data from an RCT. Neurology 83:2158–2166.

van Uffelen JG, Chinapaw MJ, van Mechelen W, Hopman-Rock M (2008) Walking or vitamin B for cognition in older adults with mild cognitive impairment? A randomised controlled trial. Br J Sports Med 42:344–351.

Woo KS, Chook P, Lolin YI, Cheung AS, Chan LT, Sun YY, Sanderson JE, Metreweli C, Celermajer DS (1997) Hyperhomocyst(e)inemia is a risk factor for arterial endothelial dysfunction in humans. Circulation 96:2542–2544.

Yiu CY, Chen SY, Yang TH, Chang CJ, Yeh DB, Chen YJ, Lin TP (2014) Inhibition of Epstein-Barr virus lytic cycle by an ethyl acetate subfraction separated from polygonum cuspidatum root and its major component, emodin. Molecules 19:1258–1272.

Zhang BK, Lai YQ, Niu PP, Zhao M, Jia SJ (2013) Epigallocatechin-3-gallate inhibits homocysteine-induced apoptosis of endothelial cells by demethylation of the DDAH2 gene. Planta Med 79:1715–1719.

Zhang CE, Tian Q, Wei W, Peng JH, Liu GP, Zhou XW, Wang Q, Wang DW, Wang JZ (2008) Homocysteine induces tau phosphorylation by inactivating protein phosphatase 2A in rat hippocampus. Neurobiol Aging 29:1654–1665.

Zhang CE, Wei W, Liu YH, Peng JH, Tian Q, Liu GP, Zhang Y, Wang JZ (2009) Hyperhomocysteinemia increases beta-amyloid by enhancing expression of gamma-secretase and phosphorylation of amyloid precursor protein in rat brain. Am J Pathol 174:1481–1491.

Zhang DM, Ye JX, Mu JS, Cui XP (2017) Efficacy of vitamin B supplementation on cognition in elderly patients with cognitive-related diseases. J Geriatr Psychiatry Neurol 30:50–59.